Virology 385 (2009) 233–244

Contents lists available at ScienceDirect

Virology

journal homepage: www.elsevier.com/locate/yviro

Role of capsid sequence and immature nucleocapsid proteins p9 and p15 in Human Immunodeficiency Virus type 1 genomic RNA dimerization

Jafar Kafaie [a,b], Marjan Dolatshahi [c], Lara Ajamian [a,b], Rujun Song [a,b], Andrew J. Mouland [a,b], Isabelle Rouiller [c], Michael Laughrea [a,b,*]

[a] McGill AIDS Center, Lady Davis Institute for Medical Research, Jewish General Hospital, Montreal, Québec, Canada H3T 1E2
[b] Department of Medicine, McGill University, Montreal, Québec, Canada H3A 2B4
[c] Department of Anatomy and Cell Biology, McGill University, Montreal, Québec, Canada H3A 2B2

ARTICLE INFO

Article history:
Received 4 October 2008
Returned to author for revision
18 October 2008
Accepted 14 November 2008
Available online 13 December 2008

Keywords:
HIV-1
RNA dimerization
Nucleocapsid protein
Capsid protein
Electron microscopy
Cores

ABSTRACT

HIV-1 genomic RNA (gRNA) dimerization is important for viral infectivity and is regulated by proteolytic processing of the Gag precursor protein (Pr55gag) under the direction of the viral protease. The processing occurs in successive steps and, to date, the step associated with formation of a wild-type (WT) level of gRNA dimers has not been identified. The primary cleavage divides Pr55gag into two proteins. The C-terminal polypeptide is termed NCp15 (NCp7–p1–p6) because it contains the nucleocapsid protein (NC), a key determinant of gRNA dimerization and packaging. To examine the importance of precursor polypeptides NCp15 and NCp9 (NCp7–p1), we introduced mutations that prevented the proteolytic cleavages responsible for the appearance of NCp9 or NCp7. Using native Northern blot analysis, we show that gRNA dimerization was impaired when both the secondary (p1–p6) and tertiary (p7–p1) cleavage sites of NCp15 were abolished, but unaffected when only one or the other site was abolished. Though processing to NCp9 therefore suffices for a WT level of gRNA dimerization, we also show that preventing cleavage at the p7–p1 site abolished HIV-1 replication. To identify the minimum level of protease activity compatible with a WT level of gRNA dimers, we introduced mutations Thr26Ser and Ala28Ser in the viral protease to partially inactivate it, and we prepared composite HIV-1 resulting from the cotransfection of various ratios of WT and protease-inactive proviral DNAs. The results reveal that a 30% processing of Pr55gag into mature capsid proteins (CA/CA-p2) yielded a WT level of gRNA dimers, while a 10% Pr55gag processing hardly increased gRNA dimerization above the level seen in protease-inactive virions. We found that full gRNA dimerization required less than 50% WT NC in complementation asssays. Finally, we show that if we destroy alpha helix 1 of the capsid protein (CA), gRNA dimerization is impaired to the same extent as when the viral protease is inactivated. Cotransfection studies show that this CA mutation, in contrast to the NC-disabling mutations, has a dominant negative effect on HIV-1 RNA dimerization, viral core formation, and viral replication. This represents the first evidence that a capsid mutation can affect HIV-1 RNA dimerization.

Introduction

The Gag and the Gag–pol polyproteins of HIV-1, also named Pr55gag and Pr160gag–pol, are rapidly processed into a common N-terminal component (the matrix–capsid-p2 polyprotein [MA–CA-p2]) and two C-terminal components: from Gag, the NCp7–p1–p6 moiety (NCp15); from Gag–pol, a polyprotein that starts with the NCp7 sequence and can include the protease-reverse-transcriptase-integrase sequence (Gowda et al., 1989; Mervis et al., 1988; Pettit et al., 2004). This and subsequent processing is achieved by the viral protease that is originally part of Pr160gag–pol and is active in both this precursor form and as a processed product (Chen et al., 2001; Pettit et al., 2004; Zybarth et al., 1994). NC designates the nucleocapsid protein (e.g. in NCp15, NCp7) or the nucleocapsid amino acid sequence within Pr55gag. NCp7 and NCp15 are typically 55 and 130 amino acids in length. NC is implicated in early infection events, such as reverse transcription of HIV-1 RNA and proviral DNA integration (e.g. Levin et al., 2005; Thomas and Gorelick, 2008), and in late viral replication events such as viral RNA dimerization, Gag–Gag multimerization, viral RNA packaging, Pr55gag processing, and virus stability (e.g. Kafaie et al., 2008).

In vitro protease assays using recombinant HIV-1 protease and Pr55gag have demonstrated that in stage 1, Pr55gag is processed into MA–CA-p2 and NCp15. In stage 2, MA–CA-p2 and NCp15 are simultaneously cleaved into MA, CA-p2, NCp9 (NCp7–p1) and p6, a reaction that is roughly 10-fold slower than stage 1. Stage 3, which is roughly 35-fold slower than stage 2, leads to the appearance of CA and NCp7 at about the same time (Fig. 1) (Erickson-Viitanen et al., 1989; Pettit et al., 1994; 2002; Wondrak et al., 1993). In this paper, a first

* Corresponding author. Fax: +1 514 340 7502.
E-mail address: mi.laughrea@mcgill.ca (M. Laughrea).

0042-6822/$ – see front matter © 2008 Elsevier Inc. All rights reserved.
doi:10.1016/j.virol.2008.11.028

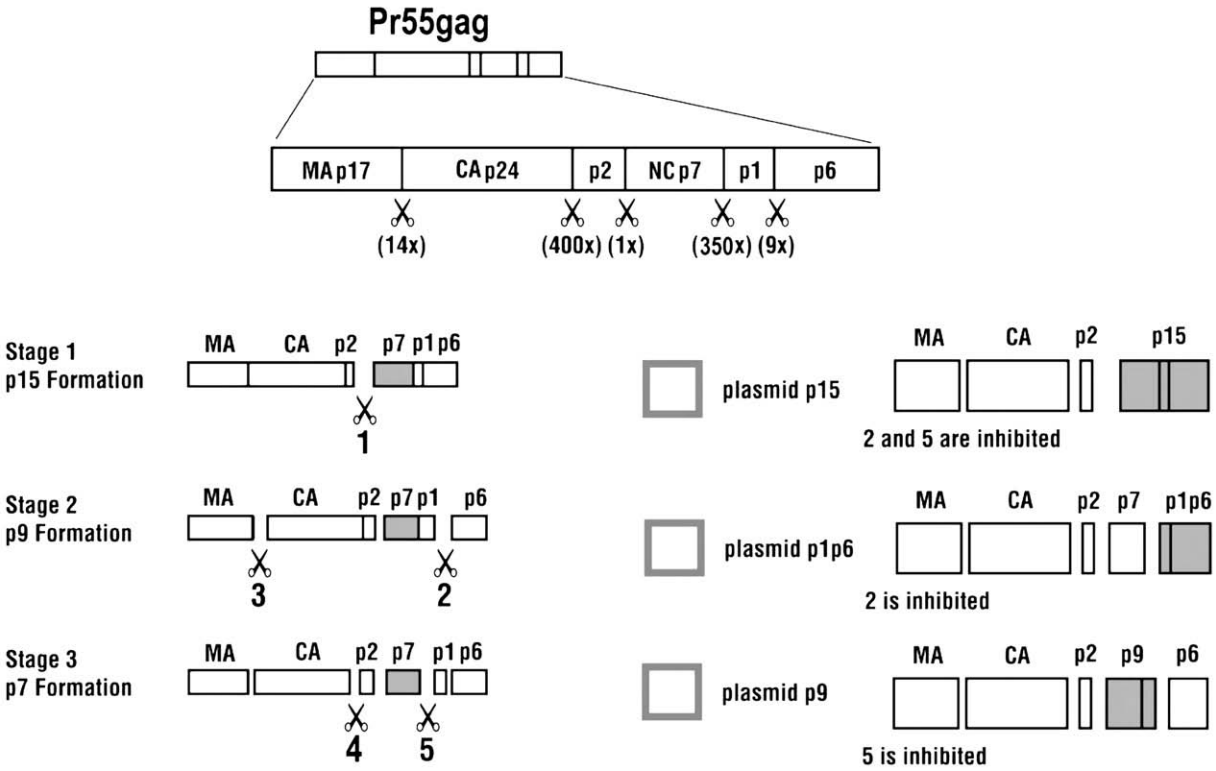

Fig. 1. Left: maturation of the HIV-1 Gag precursor polyprotein in vitro, with the five major processing sites shown as vertical lines. The rate of cleavage of each site relative to the initially cleaved p2/NC site is shown below, as determined by cleavage in vitro with recombinant protease (Pettit et al., 2002). Nx describes an N-fold reduction relative to the rate of cleavage at p2/NC. Right: illustration of the processing steps inhibited in mutants p15 (Asn55->Ser in NCp7 + Phe16->Leu in p1), p1p6 (Phe16->Leu in p1), and p9 (Asn55->Ser in NCp7).

objective is to study the role of precursor proteins NCp15 and NCp9 in HIV-1 genomic RNA (gRNA) dimerization.

NCp15 and its partial maturation product NCp9 represent 95% of the Gag and Gag–pol proteolytic intermediates containing NC (the ratio of Pr55gag to Pr160gag–pol is 20 to 1 during virus assembly). A dimeric HIV-1 gRNA appears essential for viral infectivity because, amongst other reasons, it facilitates gRNA strand exchange during reverse transcription (Song et al., 2007, 2008, and references therein). The first 55 amino acid residues of NC play key roles in gRNA dimerization (Kafaie et al., 2008; Laughrea et al., 2001), but it is not known if exercising these roles requires excision of the C-terminal peptides p1 and/or p6. Proteolytic processing of the p2-NC cleavage site is critical for HIV-1 RNA dimer maturation (Shehu-Xhilaga et al., 2001). We have pursued this line of inquiry by determining how viral RNA dimerization is affected when we abolish proteolytic processing at either the p7–p1 junction (to prevent NCp7 production), or at the p7–p1 and p1–p6 junctions (no NCp7 and no NCp9).

Additional interest in NCp15 and NCp9 comes from the study of HIV-1 strains that are resistant to antiviral protease inhibitors (PI) used in current therapies. These viruses carry mutations that reduce PI binding to the viral protease but also impair protease activity in the absence of inhibitor (Croteau et al., 1997; Rose et al., 1996b; Schock et al., 1996). This impairment is often partially relieved by Gag suppressor mutations (Carrillo et al., 1998; Zhang et al., 1997) that render the p7–p1 and/or p1–p6 junctions more scissile (Doyon et al., 1996; Mammano et al., 1998) and improve viral replication (Carillo et al., 1998; Doyon et al., 1996; Mammano et al., 1998; Zhang et al., 1997). The slow processing at the wild-type (WT) p7–p1 and p1–p6 junctions presumably becomes a replication bottleneck in PI-resistant virions. Mutations enhancing cleavage at the p7–p1 and p1–p6 junctions then get selected and propagated.

A study of the role of NCp15 and NCp9 in the viral replication cycle may clarify the reason behind the slow processing of NCp15 into NCp9 and NCp7. It may also shed light on a lifespan of NCp15 that is possibly longer than predicted from in vitro experiments. Indeed, in vivo data are consistent with the interpretation that proteolytic processing of NCp15 occurs later than the cleavage between MA and CA (Gowda et al., 1989; Kaplan and Swanstrom, 1991; Mervis et al., 1988; Veronese et al., 1987). In acutely infected CEM cells, an 80% conversion of Pr55gag into CA-p2 and CA (CA/CA-p2) was seen in the cytoplasm, but no conversion into p6 was seen (Kaplan and Swanstrom, 1991). Moreover, cleavage at the MA–CA site is RNA-independent, while NCp15 maturation is slowed-down approximately 10-fold in the absence of RNA (Sheng and Erickson-Viitanen, 1994). Thus NCp15 and CA-p2 may conceivably be processed at similar rates (the 9× of Fig. 1, derived in the presence of RNA, would then become 90×). Peptides mimicking the p1–p6 cleavage site are hydrolyzed ≥50 and ≥2-fold less efficiently than mimics of the MA–CA and CA-p2 cleavage sites, respectively (Schock et al., 1996; Tozser et al., 1991). In short, the timing of NCp15 maturation in the isolated virus is not well known, other than NCp15 is produced rather early (Chassagne et al., 1986; Gowda et al., 1989; Mervis et al., 1988; Veronese et al., 1987) and is fully processed in 3 to 4 day old HIV-1 (Henderson et al., 1992).

Though wild-type HIV-1 protease activity is probably needed for processes that might include timely capsid formation or optimal protection of gRNA against ribonucleases, full expression of other protease-dependent processes may require less than wild-type level of protease activity. A second important objective of this paper is to identify the minimal protease activity compatible with a WT level of HIV-1 RNA dimers. We introduced mutations partially inactivating the protease, and we prepared composite HIV-1

resulting from the cotransfection of various ratios of WT and protease-inactive proviral DNAs. We then studied the effect of these constructs on Pr55gag processing and gRNA dimerization in the produced viruses. A third objective is to estimate the number of WT NC sufficient for WT-like gRNA dimerization. To this end, we prepared and analyzed composite virions resulting from the cotransfection of WT and NC-disabled proviral DNAs. The results of this manuscript provide new insights into the minimal protease activity as well as the minimal NC complement needed to achieve a full level of gRNA dimerization. Finally, we have uncovered an apparent role of the capsid protein in gRNA dimerization. To add context to the results, we have also studied the effect of most mutations on gRNA packaging, virus stability and reverse transcriptase packaging.

Results

HeLa cells were transfected in parallel with equal amounts of pSVC21.BH10 or mutant proviral vectors. Proviral vector pSVC21.BH10 encodes an infectious HIV-1_{HXB2} molecular clone derived from the IIIB strain of HIV-1 (Laughrea et al., 1997). After 48 h, viruses were isolated from the culture supernatant, their capsid protein (CA) and reverse transcriptase (RT) content was measured, and their gRNA was extracted, electrophoresed on a non-denaturing agarose gel and visualized by Northern blotting with a ^{35}S-labeled HIV-1 riboprobe, followed by autoradiography. Prior to virus purification, a small volume of culture supernatant was kept to measure its CA content and determine viral replication per unit of supernatant CA (Materials and methods).

Maturation of NCp15 into NCp9 is essential for wild type like gRNA dimerization but maturation of NCp9 to NCp7 has no effect on genomic RNA dimerization and is essential for HIV-1 replication

To evaluate the activity of NCp7 precursors NCp9 and NCp15, mutants p9, p15, and p1p6 were constructed (Fig. 1 and Materials and methods). These mutants were produced by mutating the P1 positions of NCp15 (Asn55 of NCp7 and Phe16 of p1) in order to modify the rate of cleavage at the NCp7–p1 and p1–p6 sites, respectively (Pettit et al., 2002). (The P1 position is the amino acid residue immediately upstream of the scissile bond.) We were careful to choose mutations that did not interfere with the translational frameshifting site of gRNA or with the secondary structure of the downstream frameshift stimulatory stem-loop; in contrast, replacing Phe16 in p1 by serine, as found in some mutants related to our p1–p6 or p15 mutants (Coren et al., 2007; Yu et al., 1995), eliminates at least one base-pair from the frameshift stimulatory stem-loop (Dulude et al., 2002).

The level of Pr55gag processing was assessed in purified HIV-1 by immunoblotting, using antibodies against NCp7 (Fig. 2A) and CAp24 (Fig. 2B). Mutation p9 (Asn55 of NCp7 replaced by serine) blocked proteolytic maturation of NCp9 into NCp7 and p1, both in isolated viruses (Fig. 2A, lane 4; Pettit et al., 2002) and in vitro, when recombinant HIV-1 protease reacted with the Gag polyprotein (Pettit et al., 2002). Mutation p1p6 (Phe16 of p1 replaced by leucine) was designed to produce a longer-lived NCp15 intermediate (Fig. 1) that matures directly into NCp7 because it should abolish cleavage at the p1–p6 site. This implies delayed liberation of p6 from NCp15, stable attachment of p1 to the amino-terminus of p6, no production of NCp9, and unchanged timing of NCp7 appearance. Mutation p1p6

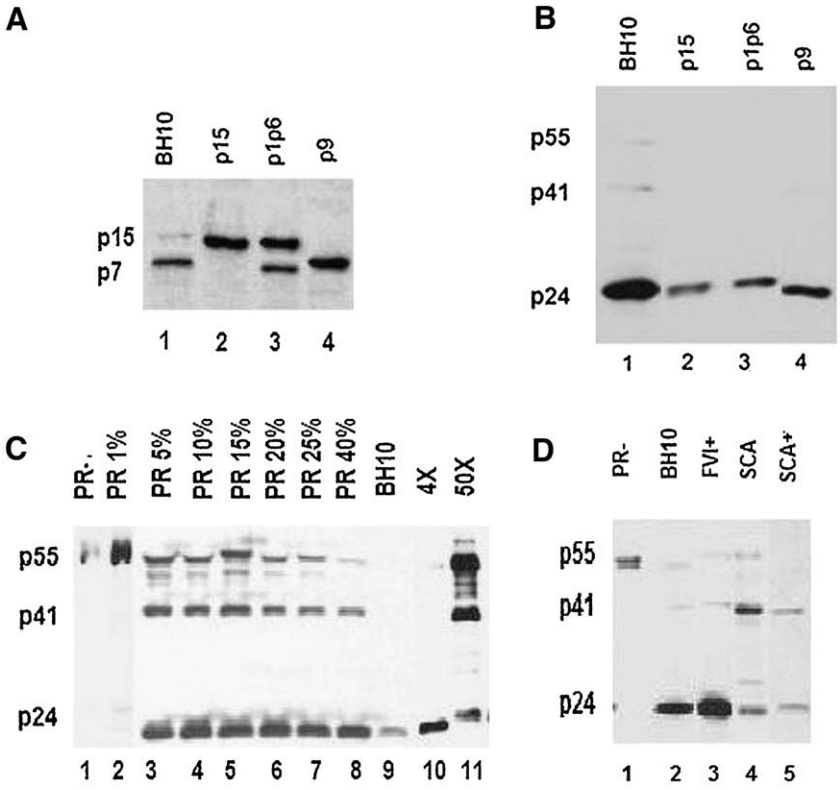

Fig. 2. Immunoblot of mutant HIV-1 preparations. Proteins were extracted from purified WT and mutant HIV-1 and analyzed by SDS gel electrophoresis. Resolved proteins were visualized using NCp7-reactive antibodies (A) or capsid protein-reactive antibodies (B, C and D). Identities of bands are indicated at the margins of the blots; p24 corresponds to CA. (A and B) Pr55gag maturation in HIV-1_{HXB2} mutated at the C-terminal Pr55gag cleavage sites. (C) Pr55gag maturation in HIV-1_{HXB2} mutated in the viral protease (PR–, 4×, 50×), or produced by the cotransfection of WT and protease-inactive proviral DNAs at ratios of 1:9 (PR 1%), 1:3.5 (PR 5%), 1:2.1 (PR 10%), 1:1.6 (PR 15%), 1:1.2 (PR 20%), 1:1 (PR 25%), and 1.7:1 (PR 40%). The apparent slower mobility of Pr55gag in lane 5 was not seen in other Western blots of PR 15% virions, and was hardly visible in longer exposures. (D) Pr55gag maturation in HIV-1_{HXB2} mutated in alpha helix 1 of the capsid protein (SCA), or produced by the cotransfection of mutant and WT proviral vectors at a ratio of 1:1 (SCA+, FVI+). FVI designates the substitution of PheVallle34 for ArgLysLys34 in the linker of the nucleocapsid protein.

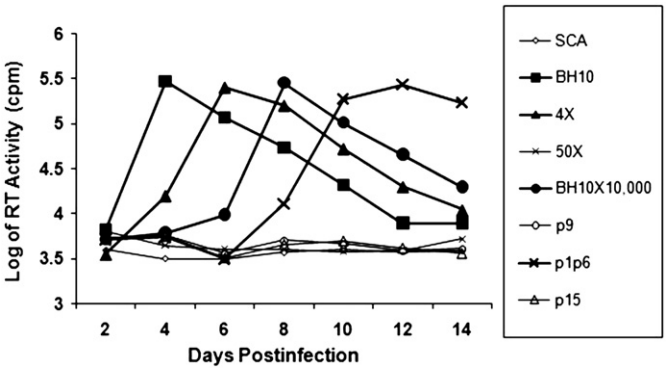

Fig. 3. Replication of HIV-1_{HXB2} mutated at the C-terminal Pr55gag cleavage sites, in residues 26–28 of the viral protease (4× and 50×) and in the capsid protein (SCA). MT2 cells were infected with an amount of undiluted progeny virus equal to 10 ng of CAp24 antigen. Virus growth was monitored by measuring reverse transcriptase activity (cpm/μl) in culture fluids at various times. The replication of 10,000-fold diluted wild-type HXB2 was also studied for comparative purposes.

prevented proteolytic maturation of NCp15 into NCp9 and p6 in vitro (Pettit et al., 2002) and in isolated viruses (Fig. 2A, lane 3). In addition, it rendered the NCp7–p1 junction less scissile. (Thus the p1p6 mutation itself, or the presence of covalently linked p6, impaired cleavage at the NCp7–p1 junction.) The result was p1p6 viruses whose NC was about 70% NCp15 and 30% NCp7 (Fig. 2A, lane 3). In comparison, only traces of NCp9 and NCp15 were visible in BH10 (Fig. 2A, lane 1). Mutation p15 was constructed by combining the p9 and p1p6 mutations (Materials and methods). The NC of the produced viruses was exclusively in the NCp15 form (Fig. 2A, lane 2), indicating that the p9 and p1p6 mutations abolished cleavage at the p7–p1 and p1–p6 junctions. In mutant p1p6, it could not be directly verified if the inhibition was as expected, for lack of an anti-p6 antibody, but the presence of large amounts of NCp15 clearly shows that the cleavage between p1 and p6 was dramatically inhibited; consistent with this is the absence of traces of NCp9 in Fig. 2A lane 3.

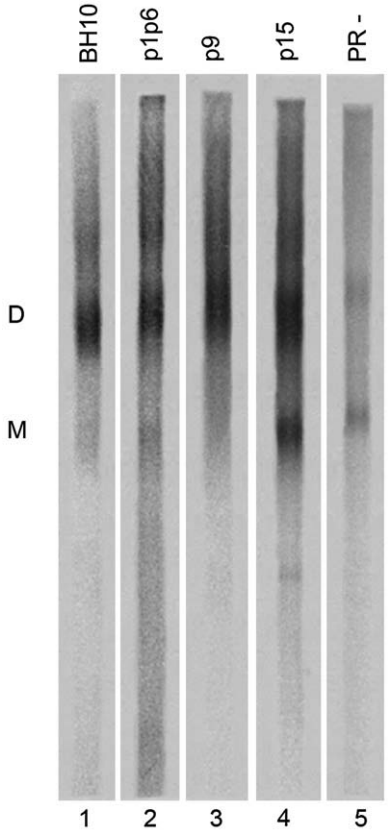

Fig. 4. Dimerization level of viral RNA isolated from HIV-1_{HXB2} mutated at the C-terminal Pr55gag cleavage sites. Genomic RNAs extracted from the respective virions were electrophoresed on a 1% non-denaturing agarose gel and analyzed by Northern blotting. The representative lanes contain viral gRNA isolated from one 100 mm tissue culture dish. D: mature dimer. M: monomer. In mutant PR−, the aspartic acid at position 25 of the viral protease active site was replaced by arginine (Song et al., 2007). This totally inactivates the protease. Note that immature dimers of the type seen in PR− HIV-1 migrate slower than WT gRNA dimers [Song et al., (2007), and references therein]. BH10 (HXB2) gRNA samples were 77% ± 0.5% dimeric (n = 29) and PR− gRNA samples were 46% ± 2.5% dimeric (n = 4). The gRNA dimerization level is independent of the amount of gRNA electrophoresed or of the concentration of DNA used in transfections (25-fold range of gRNA/proviral DNA concentrations tested (Song et al., 2007)) (not shown).

Similar amounts of CAp24 were produced by each transfected proviral DNA, indicating that the mutations created no overt assembly defect (not shown). The virion samples also did not contain appreciable amounts of Pr55gag or partially processed p41 products, indicating that the mutations in the C-terminus of Pr55gag did not alter the overall processing into CAp24 and MAp17 (Fig. 2B).

Mutations p15 and p9 abolished viral replication while p1p6 delayed the appearance of the viral production peak by 6 days (Fig. 3). Thus, viruses that are unable to cleave p1 from NCp9 exhibit dramatic replication delays.

In mutant p15, the percentage of gRNA dimerization was 76% relative to wild type level vs. 60% in protease-inactive (PR−) virions. Mutations p9 and p1p6 had little impact on gRNA dimerization (Fig. 4 and Table 1). Thus we can conclude that proteolytic maturation to NCp9 is sufficient to achieve WT gRNA dimerization yield, despite a blocked viral replication (p9 results), and that WT gRNA dimerization yield can be achieved despite a 30% complement of NCp7 and a block to the formation of NCp9 (p1p6 results). We can also conclude that free NCp15 stimulates gRNA dimerization poorly, but better than NCp15 in the context of unprocessed Pr55gag.

Genomic RNA packaging seemed unchanged by the mutations; and the mutations had no effect on RT packaging (Table 1), suggesting that normal amounts of Pr160gagpol were produced despite the location of some of them within the translational frameshift stimulatory stem-loop of gRNA. Virus stability was reduced by the p1p6 and p15 mutations but unaffected by the p9 mutation (Table 1).

Table 1
Effect of mutations introduced into the C-terminal Pr55gag cleavages sites, or inactivating the viral protease, on HIV-1 infectivity, genomic RNA dimerization, genomic RNA packaging, packaging of reverse transcriptase activity, and virus stability

	Construct name[a]	Viral replication[b]	gRNA dimerization[c]	gRNA packaging[c]	RT packaging[c]	Virus stability[c]
1	HXB2	+	100	100	100	100
2	PR−	−	60 ± 3	nd	nd	nd
3	p9	−	96 ± 2	108 ± 23	110 ± 5	120 ± 10
4	p1p6	+/−	97 ± 1	133 ± 45	115 ± 5	58 ± 5
5	p15	−	76 ± 7	106 ± 14	90 ± 7	70 ± 7

The values for HXB2 are arbitrarily set at 100, and the values for the mutants are expressed as % of wild-type level. Genomic RNA dimerization numbers were obtained by densitometric analysis. Genomic RNA packaging was measured by dot–blot hybridization. RT packaging was defined as CA-normalized RT activity: the RT activity of isolated virions divided by their CA content, relative to the ratio found in WT samples. Virus stability was defined as CA content of purified viruses divided by CA content of the culture supernatant, relative to the ratio found in WT samples (Materials and methods). nd: not done.

[a] Mutant p9, p1p6, and p15 are defined in Fig. 1. PR− is defined in Fig. 4.

[b] +: identical or close to wild type; +/−: equivalent to wild type diluted more than 10 000-fold; −: no viral replicaton detected.

[c] Margins of errors designate the standard error of 3 to 6 independent experiments for gRNA dimerization (4 on average), 2 to 5 independent experiments, for gRNA packaging (3.5 on average), and 2 independent experiments for RT packaging and virus stability.

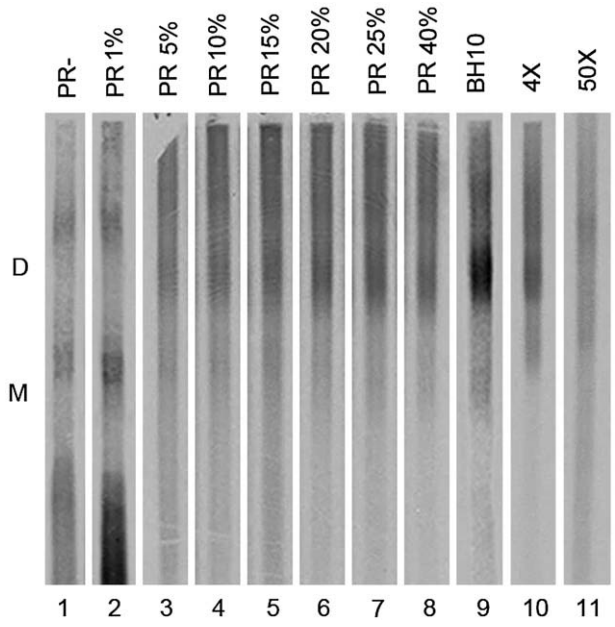

Fig. 5. Dimerization level of viral RNA isolated from HIV-1_{HXB2} mutated at residues 25 to 28 of the viral protease, or from HIV-1 produced after cotransfecting HeLa cells with wild-type and PR- proviral vectors at ratios ranging from 1:9 to 1.7:1. Experimental conditions as in Fig. 4. The "D" marks the position of mature gRNA dimers such as the dimers seen in WT virions. Dimeric gRNAs isolated from PR–, PR 1% and 50× virions have an immature, slower mobility (Materials and methods).

Wild-type gRNA dimerization yield despite a 30% CA/CA-p2 level

The minimal level of Pr55gag processing sufficient for wild-type-like gRNA dimerization is unknown. Mutations Thr26->Ser and Ala28->Ser, in the HIV-1 protease active site, reduce 4-fold and 50-fold, respectively, the catalytic activity (kcat) of recombinant protease against a decapeptide that mimics the protease-reverse-transcriptase cleavage site (Rosé et al., 1995). We inserted these mutations in the BH10 provirus to produce mutants termed 4× and 50×, respectively. Various ratios of BH10 and protease-inactive (PR−) proviral DNAs (from 1:9 to 1.7:1) were also cotransfected into cells. The resulting mutant or composite HIV-1 particles were analyzed for the ability to process Pr55gag and produce dimeric gRNAs (Figs. 2C and 5A). The mutation Asp25->Arg, in the protease active site of PR− virions, inactivates the viral protease (Gottlinger et al., 1989; Song et al., 2007), which is a member of the aspartic protease family (Davies, 1990). The composite virus particles were termed PR 1% to PR 40% (Fig. 2C; Table 2), to indicate their expected average protease activity based on simple theory (identical affinities of WT and Asp25-mutated Pr160gag–pol for each other; assembly of coexpressed viral proteins in a random way) and actual experimentation (Babé et al., 1995) (see Materials and methods).

The proportion of CA/CA-p2 was 0% of WT level in PR− virions, 5% in PR 1% virions, 11% in 50× virions, 28% in PR 5% virions, 38 to 42% in PR 10% to PR 15% virions, 70 to 81% in PR 20% to PR 40% virions, and 90% of WT level in 4× virions (Table 2). Thus a 20% expected protease activity suffices to produce viruses containing predominantly matured polyproteins, but not a 10% expected protease activity (PR 20% and PR 10% in Table 2).

In PR−, PR 1%, 50×, PR 5% and PR 20% virions, the percentage of gRNA dimers was 60, 59, 69, 92 and 95% of WT, respectively, vs. a CA/CA-p2 level of 0, 5, 11, 28 and 70% of WT (Table 2). Thus gRNA dimerization dropped from WT-like levels in PR 5% virions (28% of WT CA/CA-p2 level) to protease-inactive levels in PR 1% and 50× virions (5–10% of WT CA/CA-p2 level). Genomic RNA dimerization was not significantly improved after 50× viruses were incubated at 37 °C in cell-free growth medium for 24 h, while that seen in PR 5%, PR 10% and PR 15% viruses was undistinguishable from WT (data not shown).

50% disabled NC per virus do not impair gRNA dimerization and do not significantly impair HIV-1 replication

To gain insights into the minimum number of NC needed to achieve a WT level of gRNA dimerization in isolated viruses, HeLa cells were cotransfected with equimolar amounts of WT and NC-defective proviral DNAs. The resulting composite HIV-1 particles were analyzed for dimeric gRNA content, relative to non-composite NC-defective HIV-1. The goal was to verify if the WT NC could rescue the defective NC. NCp7 has 15 highly basic amino acid residues and only four highly acidic ones. Its central portion consists of two zinc-containing motifs (termed zinc fingers) that are 14-residue long, each, and are separated by a 7-residue linker peptide (Kafaie et al., 2008).

Five NC mutations were studied by this cotransfection protocol: ΔF1 and 3EF1 [they disabled the N-terminal zinc finger by deleting it (ΔF1) or replacing its 3 highly basic residues (Lys14, Lys20 and Arg26) by 3 glutamic acids], S3E and FVI (they disabled the linker region by replacing ArgLysLys34 by GluGluGlu34 or PheValIle34, respectively), and ΔF2 (deleted the second zinc finger). Each mutation strongly

Table 2
Effect of mutations introduced at residues 25–28 of the HIV-1 protease, and effect of cotransfected wild-type and PR- proviral vectors in ratios ranging from 1:9 to 1.7:1, on Pr55gag processing and genomic RNA dimerization

	Construct name[a]	HXB2 in cotransfection	PR− in cotransfection	Expected protease activity[b]	Pr55gag processing[c]	gRNA dimerization[c]
1	HXB2	100	0	100%	100%	100
2	PR−	0	100	0	0	60±3
3	4×	–	–	25%	92±2	97±2
4	50×	–	–	2%	11±3	69±2
5	PR 1%	10	90	1%	5±3	59±1
6	PR 5%	22	78	5%	28±6	92±2
7	PR 10%	32	68	10%	38±5	94±2
8	PR 15%	39	61	15%	42±4	94±3
9	PR 20%	45	55	20%	70±12	95±2
10	PR 25%	50	50	25%	72±8	96±2
11	PR 40%	63	37	40%	81±7	100±2

In columns 4 to 6, the values for HXB2 are arbitrarily set at 100, and the values for the mutant viruses or those produced by cotransfections are expressed as % of wild-type level. Genomic RNA dimerization numbers were obtained as in Table 1.

[a] Mutants 4× and 50× are Thr26Ser and Ala28Ser in the viral protease. PR− is defined in Fig. 4.

[b] 4× and 50×: expected protease activity based on the reaction of recombinant protease with a decapeptide substrate (Rosé et al., 1995). PR 1% to PR 40%: expected average protease activity based on the protease being active only as a dimer, on identical affinities of WT and Asp25-mutated PR160gag–pol for each other, and on assembly of coexpressed viral proteins in a random way.

[c] Margins of errors designate the standard error of 2 to 4 independent experiments for gRNA dimerization (3 on average), and 2 independent experiments for Pr55 gag processing.

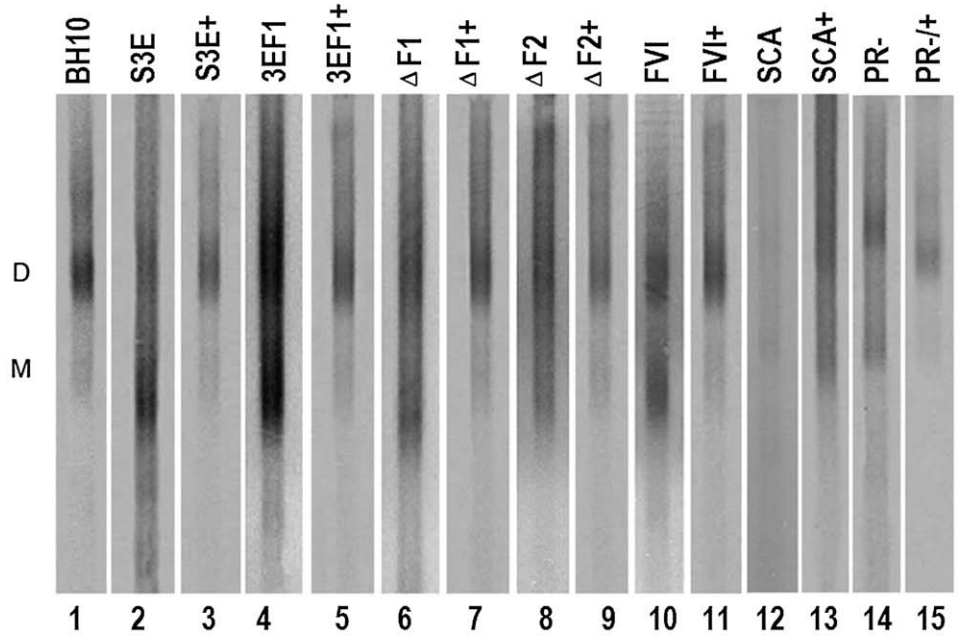

Fig. 6. Dimerization level of viral RNA isolated from viruses produced by 1:1 co-transfections of NC-mutated and HIV-1_{HXB2} proviral DNAs. Experimental conditions and interpretation of gel mobilities are as in Fig. 4 and Fig. 5. S3E+, 3EF1+, ΔF1+, (…) PR−/+ designates viruses resulting from the cotransfection of mutant (S3E, 3EF1, ΔF1, PR−, etc.) and BH10 proviral vectors.

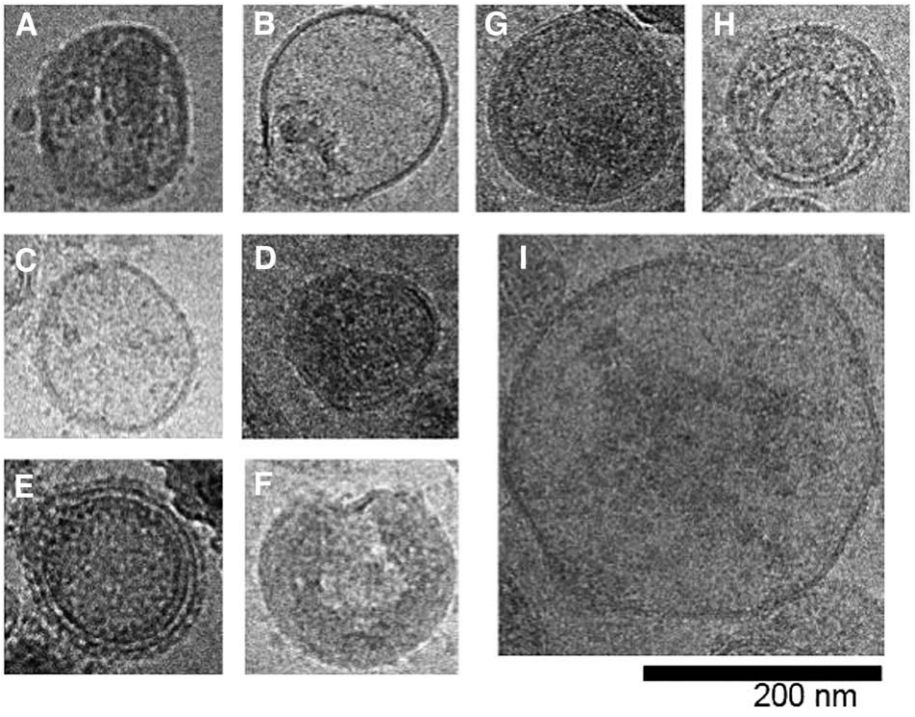

Fig. 7. Electron cryomicrographs showing the various morphologies seen in wild-type and mutant HIV-1 preparations. Ranging from 80 to 200 nm in size, HIV-1 virions were classified in Table 3 as follows:

- One layer with core: one-layer membrane particle with a significant core which is typically conical (typical example shown in a), and one-layer membrane particle, typically spherical with a usually off-centered small, irregular core (typical example shown in b).
- One-layer with no core: one-layer particle with no density inside (typical example shown in c), and particles for which it was not clear if one or several layers were present (example in d).
- Two- or multiple-layer membrane particle with no significant density inside (typical example shown in e).
- Multiple layer membrane particles in a croissant shape (typical example shown in f).
- Two-layer membrane particle with a distinct density inside (typical example in g).
- One-layer membrane particle encasing an off-centered circular membrane-like vesicle (typical example in h).
- Irregular shapes (i.e. too large, too small, or bizarre shapes such as shown in i). Scale bar equals 200 nm.

impaired gRNA dimerization in non-composite virions (Fig. 6, even numbered lanes; Kafaie et al., 2008), and abolished viral replication (Kafaie et al., 2008). However in composite HIV-1, regardless of the cotransfected NC mutation, gRNA dimerization levels were indistinguishable from those found for WT virions (Fig. 6, odd numbered lanes). This indicates that the inability of the mutant NC to properly stimulate gRNA dimerization was fully rescued by the 50% complement of WT NC. This is not due to rescue of hypothetically insufficient Pr55gag processing, because the NC mutations that were studied did not strongly affect Pr55gag processing (Kafaie et al., 2008). In addition, the inability of the NC-mutated HIV-1 to replicate was fully rescued by the 50% complement of WT NC (not shown). Since immature HIV-1 is composed of about 4000 Pr55gag polyproteins (Benjamin et al., 2005; Briggs et al., 2004), the results indicate that 2000 disabled NC per virus do not impair gRNA dimerization and do not significantly impair HIV-1 replication.

Destroying helix 1 of CA impairs gRNA dimerization, capsid formation and viral replication in a dominant negative way, in contrast to inactivating the NC linker

Mutation S3E abolishes core formation inside HIV-1 virions (Sheng et al., 1997), suggesting that interaction between NC and RNA influences virion morphology. Other NC mutations generate HIV-1 that are 80% immature in morphology, vs. 3% immature in WT (Cimarelli et al., 2000a, 2000b; Poon et al., 1996). Since NC structure influence capsid formation, we questioned whether CA structure influenced NC-directed gRNA dimerization. To address this issue, we constructed HIV-1 mutant SCA (short CA), in which residues 16 to 34 of CA were replaced by an unrelated hexapeptide HisLeuThrLeuSerSer. The purpose was to destroy the alpha helix 1 of CA and interfere with the fullerene structure of the capsid [as well as with another type of CA–CA interactions (Berthet-Colominas et al., 1999)] without impairing virus production, which depends on an intact CA C-terminal domain (Dorfman et al., 1994; Wang and Barklis, 1993). [The HIV-1 capsid appears to be largely composed of closed hexameric arrays of capsid proteins. Each CA hexamer displays an inner ring of six N-terminal domains (NTD), and an outer ring of six C-terminal domains that connects to neighboring hexamers. NTD–NTD interactions are mediated through alpha helices 1, 2 and 3 of each NTD, namely residues 17–30, 35–43, and 49–58. These form an 18-helix bundle in the center of the hexamer (Ganser-Porntillos et al., 2007; Mortuza et al., 2004)].

Not surprisingly, the SCA mutation prevented viral replication (Fig. 3). It also impaired cleavage at the MA–CA site located 15 residues upstream such that 70% of the CA of SCA virions were present in p41 form, i.e. as polyprotein MA–CA-p2 (Fig. 2D). The most intriguing finding was that SCA virions appeared nearly as gRNA dimerization defective as PR− virions. Moreover, this gRNA dimerization defect was not rescued by cotransfection with equimolar amounts of SCA and BH10 proviral DNAs. Specifically, the % of gRNA dimers was 65 ± 3% and 73 ± 2% of WT in SCA and SCA+ virions, respectively (lanes 12–14 in Fig. 6). In sharp contrast, the dimerization defects exhibited by all of the tested NC mutations were fully rescued (Fig. 6). Some gRNA bands were somewhat diffuse, but not more diffuse than what was seen in other mutants by us and others (Kafaie et al., 2008; Song et al., 2008, and references therein).

Mature HIV-1 particles contain cores consisting of a conical protein shell that is composed of about 1300 CA that encase the electron-dense gRNA dimer complexed with NC proteins (Benjamin et al., 2005; Briggs et al., 2003). Electron cryomicroscopic analysis of isolated SCA virions indicated an absence of visible cores in a majority (80–85%) of them, vs. an absence of cores in 15–20% of WT virions (Fig. 7 and Table 3). Because less than one-half of the mature CA are used to generate a core, it is conceivable that the poor core formation seen in SCA virions could be rescued by cotransfection with equimolar amounts of WT proviral DNAs. We compared the electron cryomicroscopic appearance of mutants S3E, S3E+, SCA, SCA+, PR−, and PR 25%, relative to WT. [S3E+, SCA+, PR 25% designates HIV-1 resulting from the cotransfection of mutant (S3E, SCA, PR−, respectively) and BH10 proviral vectors at a ratio of 1:1.] The results are shown in Fig. 7 and Table 3. There was no significant difference in morphology between SCA and SCA+ virions, between S3E+ and WT virions, and between PR 25% and WT virions. Both SCA and SCA+ virions were deficient in cores (~15% of virions had cores), while S3E+, PR 25% and WT virions were equally rich in cores (75–80% of virions had cores). This suggests that SCA can dominantly interfere (Herskowitz, 1987) with core formation and gRNA dimerization while S3E and PR− mutations cannot. There was a very significant difference in morphology between PR− and PR 25% virions (~0% and ~75% of virions with cores, respectively) and between S3E and S3E+ (~25% and ~75% of virions with cores, respectively). This indicates a near total rescue of core formation when S3E or PR− proviral vectors were cotransfected with BH10. Finally, SCA+ HIV-1 were replication-inactive, while S3E+ virions replicated indistinguishably from WT virions (not shown).

Discussion

In this manuscript we have examined the effects of NC and CA on HIV-1 gRNA dimerization. Our results can be summarized as follows. 1) Removal of p1 from NCp9 is not needed for a WT level of gRNA dimerization, but is essential for viral replication (p9 results; Table 1). Thus, production of NCp7 and/or free p1 is essential for HIV-1 replication but none of these 2 proteins are required for gRNA dimerization. 2) The chaperone activity of NCp15 is not sufficient for a WT level of gRNA dimerization, because NCp15 stimulates gRNA dimerization to a level intermediate between the levels seen in protease-inactive and WT viruses (p15 result). 3) The poor dimerization associated with non-maturation of NCp15 (p15 result) is rescued when the NC of HIV-1 is 70% in NCp15 form and 30% in NCp7 form

Table 3
Distribution of virion morphologies, expressed as percentage of the total number of viruses analyzed

	One-layer with core (Panels a and b, Fig. 7)	One-layer No core (Panels c and d, Fig. 7)	Two-layer No core (Panel e, Fig. 7)	Croissant shape No core (Panel f, Fig. 7)	Two-layer with core (Panel g, Fig. 7)	Off-centered No core (Panel h, Fig. 7)	Irregular shape No core (Panel I, Fig. 7)	Total number of viruses
BH10	82	3	11	1	0	2	1	194
PR−	2	7	68	4	0	15	4	138
PR 25%	75	1	14	3	0	5	2	290
S3E	27	5	53	1	0	10	4	179
S3E+(1:1)	74	2	17	2	2	2	1	210
SCA	17	47	14	2	2	12	6	258
SCA+(1:1)	12	62	7	1	2	12	5	177

The pelleted viruses from each 48-hour transfection were analyzed by electron cryomicroscopy. Particles in the microscopic field of view were analyzed by four independent observers. Two of them did not know which images corresponded to which sample. They were categorized as explained in Fig. 7. The most significant differences between the various constructs were found only within the first 3 morphological categories. Most differences within the 4 other morphological categories were non-significant. We could easily have pooled the last 4 categories into one (probably named "aberrant") because, together, they represented only 13%, on average, of BH10, PR 25%, S3E, S3E+, SCA and SCA+ virions.

(p1–p6 result). This indicates that NCp9, free p6 and free p1 are not required for gRNA dimerization. 4) A 50% complement of WT NC (1 WT NC for 1 disabled NC) suffices for a WT level of gRNA dimerization, regardless of the mutation in NC (Fig. 6). 5) A 30% Pr55gag processing into CA/CA-p2 suffices for a WT level of gRNA dimerization (PR 5% results), but a 10% processing stimulates dimerization barely more than unprocessed Pr55gag (50× results). 6) Viral replication requires processing of both NCp15 cleavage sites (Fig. 3); a WT level of gRNA dimerization requires processing at only one of these sites, no matter which one. 7) It is possible to inhibit gRNA dimerization by mutating the capsid sequence; this mutation has dominant negative effects on viral core formation, gRNA dimerization and viral replication.

The p9 mutant is intriguing because it failed to replicate. To explain this phenomenon, we note that, in vitro, NCp9 is less efficient than NCp7 or NCp15 as a nucleic acid chaperone in processes requiring both nucleic acid destabilization and nucleic acid annealing (Cruceanu et al., 2006a). Compared to NCp7 and NCp15, NCp9 is more efficient at binding and aggregating double-stranded nucleic acids (Mirambeau et al., 2006), but less efficient at rapidly binding and dissociating from nucleic acids (Cruceanu et al., 2006a). This relative inability to facilitate numerous nucleic acid rearrangements by means of a rapid kinetics of protein–nucleic acid interaction (Cruceanu et al., 2006b), may strongly disadvantage the p9 mutant in processes such as strand transfer during reverse transcription. Paradoxically, NCp9, or a variant 1 amino acid longer, can be more active than NCp7 in some RT-associated in vitro assays such as RT-directed excision repair (Bampi et al., 2006), RNase H activity of a truncated RT (Cameron et al., 1997), or recruitment of RT into nucleoprotein complexes (Lener et al., 1998).

To explain how gRNA dimerization was impaired in the p15 mutant, we note that NCp15 has as much affinity for single-stranded nucleic acids as NCp7 (Cruceanu et al., 2006a) but is inefficient at aggregating nucleic acids, no matter whether they are single-stranded or double-stranded (Mirambeau et al., 2006). This deficiency is consistent with the poor production of gRNA dimers seen in p15 virions.

The replication defect of the p1–p6 mutant is in good agreement with replication defects previously observed with two different p1–p6 cleavage mutants (Yu et al., 1995; Coren et al., 2007). A severe defect during or just before proviral DNA integration has been noted in p15 and p1–p6 cleavage mutants comparable to ours (Coren et al., 2007). It has been suggested that a lack of NCp9 was responsible for this integration defect (Coren et al., 2007).

Putting together our results and Song et al. (2007), it follows that a 30% level of CA/CA-p2 in grown-up viruses (48 h post transfection) yields a greater level of gRNA dimers than an 80% level of CA/CA-p2 in newly released viruses (Song et al., 2007). [In newly released HIV-1, the percentage of gRNA dimers was 80% of the level seen in >2 h old HIV-1 (Song et al., 2007).] To reconcile these results, we suggest that gRNA dimerization yield responds neither instantaneously nor within minutes to the number of processed Pr55gag made available by the virus. The proportion of gRNA dimers would depend on a combination of the number of processed Pr55gag available plus the time (in tens of minutes or in hours) they had to act on gRNA. A large number of processed Pr55gag can dimerize gRNA in a short time (Song et al., 2007); but a smaller number can achieve the same or better results albeit in viruses that are many hours older (this paper). It would be interesting to know the earliest age at which PR 5% HIV-1 contain a mature level of gRNA dimers. Given the contrast between the effects of a 10% and a 30% CA/CA-p2 level on gRNA dimerization, it seems possible that the gRNA of 6 h old PR 5% virions may be less dimeric than in newly released virions.

Our data are consistent with previous experiments showing that a 20% complement of WT NC suffices for a WT level of gRNA packaging (Schwartz et al., 1997), and that sequential passaging of an HIV-1_{NL4-3} mutant similar to the p9 mutant restored the NCp7–p1 site within 4 weeks (Coren et al., 2007). The latter result supports our finding that proteolytic processing at the NCp7–p1 junction is essential for HIV-1_{HXB2} replication (Fig. 3). The HIV-1_{NL4-3} mutant, however, replicated much faster than the p9 mutant. It is known that some mutations in NC, though less than a majority of them, impair HIV-1_{HXB2} more than HIV-1_{NL4-3} (Cimarelli and Luban, 2001; Kafaie et al., 2008). Note also that substituting leucine for Phe16 of p1 in HIV-1_{HXB2} impeded cleavage at the upstream NCp7–p1 junction (p1p6 result), while substituting serine did not, in HIV-1_{NL4-3} (Coren et al., 2007).

Reducing the proportion of CA/CA-p2 to 80–85% of WT level, by means of suboptimal PI concentrations, does not impair gRNA dimerization (Moore et al., 2008), and correlates with altered virion morphology, notably the presence of electron dense material on one side, rather than in or near the center, of the virus particle (Kageyama et al., 1994; Kaplan et al., 1993; Moore et al., 2008). Our data were obtained by means of protease mutations or cotransfection studies, and they extend these results by showing that a 30% —but not a 10%— level of CA/CA-p2 is compatible with full gRNA dimerization.

Why is the mature CA level higher than the expected protease activity? Namely, why is there a 5% CA/CA-p2 level in PR 1% virions, a 28% level in PR 5% virions, and a 70% level in PR 20% virions, when the protease activity of PR 1%, 5%, and 20% virions is expected to be 1%, 5%, and 20% of WT, respectively? The answer is most likely that protease-directed Pr55gag maturation is completed in WT long before viruses reach 48 h of age, but is still in the linear range of its kinetics in mutant 50× and in most virions resulting from cotransfected PR− and WT proviral DNAs. Given that PR 20% HIV-1 yield a 70% CA–CA-p2 level, and assuming linearity of Pr55gag processing kinetics over the range PR 1% to 20%, it follows that PR 10%, 5% and 1% cotransfections should yield 35%, 18% and 4% processing levels. This is not significantly different from to the 38%, 28% and 5% that were experimentally seen (Table 2).

Since Pr55gag processing was more complete in 4× HIV-1 than in PR 40% HIV-1 (Fig. 2C; Table 2), the Thr26Ser protease mutant might have been better termed 2× rather than 4×, to reflect our observation that its protease activity seems to be at least 50% of WT. This is supported by the finding that the kcat of the 4× recombinant HIV-1 protease is only 1.5-fold lower than WT against a peptide mimicking the CA-p2 junction (Konvalinka et al., 1995). In agreement with our results, CA/CA-p2 levels of <10% and 80–90% of WT were previously reported for 50× (Rosé et al., 1995) and 4× virions (Konvalinka et al., 1995; Rosé et al., 1995), respectively.

Several results (e.g. large gRNA dimerization yield in PR 5% virions; rescue of gRNA dimerization by a 50% complement of WT NC) indicate that mutant and BH10 Pr55gag/Pr160gag–pol polyproteins produced by cotransfection do not assemble separately. The results are compatible with assembly of the coexpressed mutant and BH10 polyproteins in a wholly or partly random way.

We have shown that deleting alpha helix 1 of CA, and some adjacent residues, profoundly compromises HIV-1 in its ability to dimerize gRNA. This represents the first evidence that a capsid mutation can affect gRNA dimerization. This surprising effect is probably not due to the considerable presence of p41 in the SCA mutant, because specifically blocking processing at the MA–CA cleavage site does not impair gRNA dimerization (Shehu-Xhilaga et al., 2001), though it results in virions containing no conical capsid shell (Gottlinger et al., 1989). The poor gRNA dimerization seen in SCA virions may be related to the inability of the SCA mutation to efficiently stimulate core formation. This inability morphologically distinguishes SCA virions from HIV-1 specifically unable to process the MA–CA cleavage site (Gottlinger et al., 1989). Since the HIV-1 capsid shell is 5 to 10 times less voluminous than the virus (Benjamin et al., 2005; Briggs et al., 2003), and since unstructured cores are >10 times less voluminous than the virus, the concentration of gRNA in the SCA mutant may be an order of magnitude lower than in WT. The same may befall NCp15/p9/p7, if they are assumed enclosed by the capsid in

Table 4
Primers used to introduce intended mutations in HIV-1HXB2

Construct name	Primer (all primers are sense)
p9	5′gattgtactgagagacaggcttctttttagggaagatctggccttcc
p1p6	5′cctacaagggaaggccagggaatcttcttcagagcagaccagagccaac
4×	5′ctaaaggaagctctattagattcaggagcagatgatacag
50×	5′ggaagctctattagatacaggatcagatgatacagtattagaag

All primers were synthesized by ACGT corp. in Toronto (Canada).

WT. Alternatively, the SCA mutation may act on gRNA dimerization at the RNA level. However this seems unlikely because it would contradict the current understanding that there is no gRNA dimerization site located 3′ of nt 500 (the midmatrix section) of gRNA (Song et al., 2008). SCA may also have an idiosyncratic effect: in addition to inactivating a function of the WT capsid protein, it may endow CA with an interfering activity unconnected to the native function of CA.

Point mutations in alpha helices 1–3 of the NTD of CA (e.g. R18A/N21A, A22D, E28A/E29A, M39D, A42D, D51A) prohibit formation of conical capsids, but may allow formation of more or less distinct cores in HIV-$_{NL4-3}$ (Von Schwedler et al., 1998, 2003). Similarly, mutations W23A, F40A and D51A (Tang et al., 2001), deletion of residues 19–21 (Dorfman et al., 1994), or small insertions between amino acid residues 11/12, 19/21 or 51/52 of CA (Reicin et al., 1996) result in particles containing no cone-shaped cores, and even no defined cores in the case of W23A (Tang et al., 2001). It will be interesting to verify whether smaller mutations in helices 1 or 2 of CA, such as the point mutations studied by Tang et al. (2001), or Von Schwedler et al. (2003), impair gRNA dimerization.

Materials and methods

Plasmid construction

Proviral vector pSVC21.BH10 encodes a HIV-1$_{HXB2}$ cDNA clone. Mutant proviral vectors, except p15, were constructed from pSVC21.BH10 by PCR mutagenesis, using primers described in Table 4. The nucleotide positions are based on the sequence of HIV-1 gRNA. To prepare mutants p9, p1p6, 4× and 50×, a DNA fragment extending from Apa I to Bcl restriction sites (Amersham) was synthesized with the desired mutations by PCR, and ligated into pSVC21.BH10. Mutant p15 was constructed from mutant p9, using the primers for the p1p6 mutant. The PCR-produced DNA fragment was then ligated into pSVC21.BH10. To prepare mutant SCA, restriction sites Nar I and Spe I were used with the primers depicted in Table 4. After mutagenesis and ligation, all mutated DNA fragments produced by PCR were completely sequenced (ACGT Inc., Toronto) to verify that the desired mutation, and no other mutation, was introduced by the mutagenic procedure.

Cell culture and transfections

HeLa Cells were cultured at 37 °C in a medium consisting of Dulbecco's modified Eagle's medium (DMEM), 10% fetal calf serum, ampicillin and streptomycin (Invitrogen). The PolyFect transfection reagent (Qiagen) was used to transfect 9 μg of proviral DNA into 50% to 70% confluent HeLa cells in 100- by 20-mm petri dishes containing 10 ml of culture medium. In cotransfections, the total amount of proviral DNA transfected remained 9 μg.

Calculation of expected protease activity in composite HIV-1

Viruses produced by cotransfection cannot be uniform in composition, even if all coexpressed viral proteins could coassemble in a random way. However, the larger the number of transcribed proviral DNAs per successfully transfected cell, the smaller the variance in composition will be. Transfected HeLa cells typically contain 10^5 exogenous plasmids per cell and 10^3 exogenous plasmids per nucleus (Ludtke et al., 2002; Tseng et al., 1997; Vaughan et al., 2006)). This may translate into ~300 transcribed proviral DNAs per successfully transfected cell, based on observing that microinjection of 3 protein-coding plasmids per nucleus generates detectable amounts of exogenous proteins in ≥50% of microinjected HeLa cells (Ludtke et al., 2002). Assuming identical affinities between WT and Asp25-mutated Pr160gag–pol (Babé et al., 1995), and random coassembly of the coexpressed viral proteins, the names we gave to the composite protease-defective HIV-1 (PR 1%, PR 5%, etc.) should closely represent the average protease activity of the HIV-1 population produced by cells containing ≥40 transcribed proviral DNAs. If there were only 10 transcribed proviral DNAs per cell, PR 1%, PR 25% and PR 40% HIV-1 would only need to be renamed PR 1.9%, PR 28% and PR 50%, respectively (Spiegel, 1961). These alternative numbers would not change any conclusion of this paper.

The HIV-1 protease is active only as a dimer, and each monomer contributes, via Asp25, one of the two catalytic aspartic acid residues required in the active site of the enzyme (Babé et al., 1995; Dilanni et al., 1990; Krausslich, 1991; Rose et al., 1996a). Thus the protease activity yielded by the coexpression of BH10 and PR− proviral DNAs is related to the proportion of WT protease dimers in the composite viruses. For example, cotransfection of BH10 and PR− proviral DNAs at a 1 to 1 ratio and assembly of synthesized viral proteins in a random way should yield an activity that is 25% of WT on average (Babé et al., 1995), or barely larger (see above), even though, statistically, a minority of produced viruses contain an equal number of WT and Asp25-mutated proteases (a minority of successfully transfected cells will contain an equal number of BH10 and PR− proviral DNAs, but on average they will).

Viral replication assay

Mutant proviruses and the parental BH10 provirus were independently transfected into HeLa cells. Virus-containing supernatants were collected 48 h post-transfection and passed through 0.2 μm pore-size cellulose acetate filters to remove the cells. The CAp24 content of these clarified supernatants was measured using an ELISA kit (Vironostika HIV-1 Antigen, Biomerieux). Equal amount of the supernatants (10 ng of CAp24 content) were used to infect equal numbers of MT2 cells (6×10^6 cells in 10 ml of RPMI 1640 medium, 10% fetal calf serum, ampicillin and streptomycin (Invitrogen), per petri dish). In the human T-cell line MT2, only a short time lag separates infection from viral replication (Harada et al., 1985). After 2 h, cells were washed twice to remove unbound viruses and were then maintained in serum-supplemented medium. On every other day, cells were diluted 1 in 2 into fresh medium and the RT activity in the supernatant of the removed medium was determined. RT activity measurements were made over a period of 14 days.

RT activity

The exogenous (oligo (dT) directed) RT activity was measured by adding 40 μl of RT cocktail (60 mM Tris–HCl [pH 7.9], 180 mM KCl, 6 mM $MgCl_2$, 6 mM dithiothreitol, 0.6 mM EGTA, 0.12% Triton X-100, 6 μg/ml oligo (dT), 12 μg/ml poly(rA), 0.05 mM 3 H dTTP) to a 10 μl sample. After incubation for 2 h at 37 °C, the reaction was stopped with cold 10% TCA (150 μl per well), and precipitated for 30 min at 4 °C. The precipitate was blotted, washed and scintillation counted.

Virus purification and isolation of HIV-1 viral RNA

Filtered virus-containing supernatants were centrifuged (SW41 rotor, 35 000 rpm, 4 °C, 1 h), through a 2 ml 20% (w/v) sucrose cushion in phosphate-buffered saline (PBS). The virus pellet was dissolved in 400 μl sterile lysis buffer [50 mM Tris (pH7.4), 50 mM NaCl, 10 mM

EDTA, 1% (w/v) SDS, 50 μg tRNA per ml, and 100 μg proteinase K per ml], and extracted twice at 4 °C with an equal volume of buffer-saturated phenol–chloroform–isoamylalcohol (25:24:1) (Invitrogen). The aqueous phase was precipitated overnight at −80 °C with 0.1 volume of 3 M sodium acetate (pH 5.2) and 2.5 volumes of 95% ethanol, and centrifuged at 14,000 rpm in an Eppendorf 5145 micro centrifuge at 4 °C for 30 min. The gRNA pellet was rinsed with 70% ethanol, and dissolved in 10 μl buffer S (10 mM Tris (pH 7.5), 100 mM NaCl, 10 mM EDTA and 1% SDS) (Song et al., 2007).

Electrophoretic analysis of HIV-1 gRNA

The gRNA was electrophoresed under non-denaturing conditions and identified by Northern (RNA) blot analysis (Song et al., 2007). Electrophoretic conditions were 4 V/cm for 4 h on a 1% (w/v) agarose gel in TBE2 (89 mM Tris, 89 mM Borate and 2 mM EDTA, pH 8.3) at 4 °C. After electrophoresis, the gel was heated at 65 °C for 30 min in 10% (w/v) formaldehyde, and the embedded RNAs were diffusion transferred to a Hybond N+ nylon membrane (Amersham). After drying at room temperature for 2 h, crosslinking (3000 j in a UV Stratalinker), and prehybridization at 42 °C for 3 h in 6× SSPE (1× SSPE is 0.15 M NaCl, 10 mM NaH2PO4, and 1 mM EDTA {pH 7.4}), 50% (w/v) deionized formamide, 10% dextran sulfate, 1.5% SDS, 5× Denhardt's reagent, 100 μg/ml salmon sperm DNA, the membrane was hybridized overnight in prehybridization buffer devoid of Denhardt's reagent in a rotating hybridization oven at 42 °C to approximately 25 μCi of ^{35}S-labeled antisense RNA 636–296 (a 356-nt RNA that is the antisense of the 296 to 636 region of the HIV-1 genome prepared with the SP6 Megascript kit [Ambion]) (Laughrea and Jetté, 1996). This was followed by two 30 min washes in 1× SSC [1× SSC is 0.15 M NaCl plus 0.015 M sodium citrate]– 0.1% SDS at room temperature and 37 °C, and one 30 min wash in 0.2× SSC–0.1% SDS at 45 °C (Laughrea et al., 1997), exposure to a Kodak BioMax MR X-ray film, and densitometric analysis.

Densitometric analysis

The autoradiograms were scanned and analysed with the NIH 1.6.3 program. Care was taken to scan variously exposed films to guard against over-exposed or under-exposed bands or spots. The monomer and dimer bands were considered of equal width. That width was approximately twice the vertical size of the D and M letters used to indicate dimers and monomers in the relevant figures. Material located elsewhere in the gels was not taken into account in the calculation of the percentage of dimers. On the left side of each Northern blot, "D" indicates the position of WT (i.e. mature) gRNA dimers. Genomic RNA dimers from PR 1% and 50× virions migrated 20% slower than WT gRNA dimers, and were therefore located above the "D" marker. In other words, they migrated like PR− gRNA dimers (Song et al., 2007, and references therein), which are also called immature dimers. The portion of the densitometric profile taken as representing the dimer or monomer band was centered on the peak of dimer or monomer intensity, no matter the respective positions of the dimer and monomer peaks. The diffuse character of many bands may reflect conformational diversity among the gRNA molecules. It is not due to poor resolution of the gels because heat denatured gRNAs formed a sharp band at the monomer position (not shown).

Genomic RNA packaging

The amount of gRNA per unit CAp24 of virus was quantitated by hybridization with antisense RNA 636–296 using a dot–blot assay. Virus pellets were resuspended in 400 μl of Trizol LS reagent (Invitrogen), and incubated at 30 °C for 5 min. 100 μl of chloroform was added, followed by shaking for 15 s and incubation at room temperature for 15 min. After centrifugation (12,000 ×*g*, 15 min, 4 °C), the colorless aqueous upper phase was mixed with 250 μl of isopropyl alcohol, incubated at room temperature for 10 min and centrifuged again. The precipitated RNA was washed once with 500 μl of 70% ethanol, pelleted (7500 ×*g*, 5 min, 4 °C), air-dried, dissolved in 10 μl RNase-free water and stored at −20 °C. Serial 10-fold dilutions of wild type RNA samples, normalized for input virion CAp24, were used to construct a standard curve. 29 μl of buffer F (100% deionized formamide, 20 μl; 20× SSC, 2 μl; 37% formaldehyde, 7 μl) was added to each sample, followed by incubation (68 °C, 15 min) and chilling on ice. After adding 78 μl of 20× SSC buffer, samples were vacuum-suction transferred to a Hybond N+ nylon membrane (Amersham) sandwiched within a Hybri-Dot filtration manifold (Bethesda Research Laboratories). The wells were washed twice with 1 ml of 10× SSC, and suction continued for a further 5 min to dry the membrane. The membrane was removed, dried for 4 h, cross-linked, pre-hybridized, hybridized, autoradiographed and scanned as for Northern blot analysis (above). To confirm the scans, each individual spot of the nylon membrane was excised and scintillation counted.

Virus stability and RT packaging

1.2 ml of filtered virus-containing supernatant was pelleted through a 0.3 ml 20% sucrose cushion in the TL-100 Beckman ultracentrifuge (TLA 55 rotor, 45,000 rpm, 1 h, 4 °C). The virus pellet was dissolved in 10 μl of PBS and its CAp24 content was measured using an ELISA kit (Vironostika HIV-1 Antigen, Biomerieux). The CA content of the purified viruses divided by the CA content of the 48 h culture supernatant, relative to the ratio found in WT, was taken as a measure of virus stability (Wang and Aldovini, 2002; Wang et al., 2004). The ratio pellet/supernatant was 0.43±0.07 in WT (this was taken to mean 100 in Table 1).

The exogenous RT activity of the pelleted viruses divided by their CA content, relative to the ratio found in WT, was interpreted as RT packaging.

Immunoblots and Pr55gag proteolytic maturation

At 48 h post-transfection, cells were lysed in ice-cold NP-40 containing buffer (100 mM NaCl, 10 mM Tris, 1 mM EDTA, 0.5% NP-40, and protease inhibitor cocktail [Roche]). Supernatants were cleared by centrifugation at 3000 ×*g* and filtered (0.22 μm). Viruses were then concentrated through a sucrose cushion by ultracentrifugation. Equal amounts of viruses (judged by CAp24-ELISA) were lysed in the above buffer and subjected to SDS-polyacrylamide gel electrophoresis. Viral proteins were detected by immunoblotting using an enhanced chemiluminescence immunoblot detection kit (Amersham). A rabbit anti-capsid antibody (ABT-Trinity Biotechnology, CA, USA), as well as a rabbit NCp7 antiserum (kind gift from R. J. Gorelick), were used for protein recognition. The signals for CA-containing or NC-containing proteins were quantitated by densitometric scanning and analysed with the NIH 1.6.3 program. The signal obtained from the CA/CA-p2 band was divided by the total signal obtained from all CA-containing proteins, to calculate what is reported as Pr55gag processing level.

Electron cryomicroscopy

5 μl of purified viruses were added to glow-discharged EM holey carbon grids and were blotted and frozen hydrated by plunging into a bath of liquid ethane slush (Dubouchet et al., 1988). They were stored under liquid nitrogen temperature until transfer to a 626 Single Tilt Cryotransfer System (Gatan Inc.) and observed with a FEI G2 F20 cryo-STEM microscope operated at 200 kV (FEI, Inc). Images were recorded on a Gatan Ultrascan 4k×4k Digital (CCD) Camera System Camera at a nominal magnification of 29,000× at a defocus level of −2.5 to −3.5 μm.

Acknowledgments

We thank Mohammed Jalalirad for useful discussions, Robert J. Gorelick for the kind gift of antibodies, Mark A. Wainberg for access to the HIV-1 growth facility, and Amrit Kirpalani and Alice (Xiao Fan) Zhang for help in the EM classification. L. A. is a recipient of a Doctoral Research Award from the CIHR. A.J.M. is recipient of a CIHR New Investigator and FRSQ Chercheur-boursier awards. I.R. is recipient of a CIHR New Investigator award. This work was supported by CIHR group grant 13918, by CIHR grant #MOP-12312 to M.L., by CIHR grant # MOP-38111 to A.J.M., and by CIHR grant #MOP-86693 to I.R.

References

Babé, L.M., Rosé, J., Craik, C.S., 1995. Trans-dominant inhibitory human immunodeficiency virus type 1 protease monomers prevent protease activation and virion maturation. Proc. Natl. Acad. Sci. U. S. A. 92, 10069–10073.

Bampi, C., Bibillo, A., Wendeler, M., Divita, G., Gorelick, R.J., Le Grice, S.F.J., Darlix, J.-L., 2006. Nucleotide excision repair and template-independent addition by HIV-1 reverse transcriptase in the presence of nucleocapsid protein. J. Biol. Chem. 281, 11736–11743.

Benjamin, J., Ganser-Pornillos, B.K., Tivol, W.F., Sundquist, W.I., Jensen, G.J., 2005. Three-dimensional structure of HIV-1 virus-like particles by electron cryotomography. J. Mol. Biol. 346, 577–588.

Berthet-Colominas, C., Monaco, S., Novelli, A., Sibai, G., Mallet, F., Cusack, S., 1999. Head-to-tail dimers and interdomain flexibility revealed by the crystal structure of HIV-1 capsid protein (p24) complexed with a monoclonal antibody Fab. EMBO J. 18, 1124–1136.

Briggs, J.A.G., Wilk, T., Welker, R., Krausslich, H.-G., Fuller, S.D., 2003. Structural organization of authentic, mature HIV-1 virions and cores. EMBO J. 22, 1707–1715.

Briggs, J.A.G., Simon, M.N., Gross, I., Krausslich, H.G., Fuller, S.D., 2004. The stoichiometry of Gag protein in HIV-1. Nat. Struct. Mol. Biol. 11, 672–675.

Cameron, C.E., Ghosh, M., Le Grice, S.F.J., Benkovic, S.J., 1997. Mutations in HIV reverse transcriptase which alter RNase H activity and decrease strand transfer efficiency are suppressed by HIV nucleocapsid protein. Proc. Natl. Acad. Sci. U. S. A. 94, 6700–6705.

Carrillo, A., Stewart, K.D., Sham, H.L., Norbeck, D.W., Kohlbrenner, W.E., Leonard, J.M., Kempf, D.J., Molla, A., 1998. In vitro selection and characterization of human immunodeficiency virus type 1 variants with increased resistance to ABT-378, a novel protease inhibitor. J. Virol. 72, 7532–7541.

Chassagne, J., Verrelle, P., Dionet, C., Clavel, F., Barre-Sinoussi, F., Chermann, J.C., Montagnier, L., Gluckman, J.C., Klatzmann, D., 1986. A monoclonal antibody against LAV gag precursor: use for viral protein analysis and antigenic expression in infected cells. J. Immunol. 136, 1442–1445.

Chen, N., Morag, A., Almog, N., Blumenzweig, I., Dreazin, O., Kotler, M., 2001. Extended nucleocapsid protein is cleaved from the Gag–Pol precursor of human immunodeficiency virus type 1. J. Gen.Virol. 82, 581–590.

Cimarelli, A., Sandin, S., Hoglund, S., Luban, J., 2000a. Basic residues in human immunodeficiency virus type 1 nucleocapsid promote virion assembly via interactions with RNA. J. Virol. 74, 3046–3057.

Cimarelli, A., Sandin, S., Hoglund, S., Luban, J., 2000b. Rescue of multiple viral functions by a second-site suppressor of a human inmunodeficiency virus type 1 nucleocapsid mutation. J. Virol. 74, 4273–4283.

Cimarelli, A., Luban, J., 2001. Context-dependent phenotype of a human immunodeficiency virus type 1 nucleocapsid mutation. J. Virol. 75, 7193–7197.

Coren, L.V., Thomas, J.A., Chertova, E., Sowder II, R.C., Gagliardi, T.D., Gorelick, R.J., Ott, D. E., 2007. Mutational analysis of the C-terminal Gag cleavage sites in human immunodeficiency virus type 1. J. Virol. 81, 10047–10054.

Croteau, G., Doyon, L., Thibeault, D., McKercher, G., Pilote, L., Lamarre, D., 1997. Impaired fitness of human immunodeficiency virus type 1 variants with high-level resistance to protease inhibitors. J. Virol. 71, 1089–1096.

Cruceanu, M., Urbaneja, M.A., Hixson, C.V., Johnson, D.G., Datta, S.A., Fivash, M.J., Stephen, A.G., Fisher, R.J., Gorelick, R.J., Casas-Finet, J.R., Rein, A., Rouzina, I., Williams, M.C., 2006a. Nucleic acid binding and chaperone properties of HIV-1 Gag and nucleocapsid proteins. Nucl. Acids Res. 34, 593–605.

Cruceanu, M., Gorelick, R.J., Musier-Forsyth, K., Rouzina, I., Williams, M.C., 2006b. Rapid kinetics of protein–nucleic acid interaction is a major component of HIV-1 nucleocapsid protein's nucleic acid chaperone function. J. Mol. Biol. 363, 867–877.

Davies, D.R., 1990. The structure and function of the aspartic proteinases. Ann. Rev. Biophys. Biophys. Chem. 19, 189–215.

Dilanni, C., Davis, L., Holloway, M., Herber, W.K., Darke, P.L., Kohl, N.E., Dixon, R.A., 1990. Characterization of an active single polypeptide form of the human immunodeficiency virus type 1 protease. J. Biol. Chem. 265, 17348–17354.

Doyon, L., Croteau, G., Thibeault, D., Poulin, F., Pilote, L., Lamarre, D., 1996. Second locus involved in human immunodeficiency virus type 1 resistance to protease inhibitors. J. Virol. 70, 3763–3769.

Dorfman, T., Bukovsky, A., Ohagen, A., Hoglund, S., Gottlinger, H.G., 1994. Functional domains of the capsid protein of human immunodeficiency virus type 1. J. Virol. 68, 8180–8187.

Dubouchet, J., Adrian, M., Chang, J.J., Homo, J.C., Lepault, J., McDowall, A.W., Schultz, P., 1988. Cryo-electron microscopy of vitrified specimens. Q. Rev. Biophys. 21, 129–228.

Dulude, D., Baril, M., Brakier-Gingras, L., 2002. Characterization of the frameshift stimulatory signal controlling a programmed -1 ribosomal frameshift in the human immunodeficiency virus type 1. Nucleic Acids Res. 30, 5094–5102.

Erickson-Viitanen, S., Manfredi, J., Viitanen, P., Tribe, D.E., Tritch, R., Hutchison III, C.A., Loeb, D.D., Swanstrom, R., 1989. Cleavage of HIV-1 gag polyprotein synthesized in vitro: sequential cleavage by the viral protease. AIDS Res. Hum. Retroviruses 5, 577–591.

Ganser-Pornillos, B.K., Cheng, A., Yeager, M., 2007. Structure of full-length HIV-1 CA: a model for the mature capsid lattice. Cell 131, 70–79.

Gottlinger, H.G., Sodroski, J.G., Haseltine, W.A., 1989. Role of capsid precursor processing and myristoylation in morphogenesis and infectivity of human immunodeficiency virus type 1. Proc. Natl. Acad. Sci. U. S. A. 86, 5781–5785.

Gowda, S.D., Stein, B.S., Engleman, E.G., 1989. Identification of protein intermediates in the processing of the p55 HIV-1 gag precursor in cells infected with recombinant vaccinia virus. J. Biol. Chem. 264, 8459–8462.

Harada, S., Koyanagi, Y., Yamamoto, N., 1985. Infection of HTLV III/LAV in HTLV-I-carrying cells MT-2 and MT-4 and application in a plaque assay. Science 229, 563–566.

Henderson, L.E., Bowers, M.A., Sowder II, R.C., Serabyn, S.A., Johnson, D.G., Bess, J.J., Arthur, L.O., Bryant, D.K., Fenselau, C., 1992. Gag proteins of the highly replicative MN strain of human immunodeficiency virus type 1: posttranslational modifications, proteolytic processings, and complete amino acid sequences. J. Virol. 66, 1856–1865.

Herskowitz, I., 1987. Functional inactivation of genes by dominant negative mutations. Nature 329, 219–222.

Kafaie, J., Song, R., Abrahamyan, L., Mouland, A.J., Laughrea, M., 2008. Mapping of nucleocapsid residues important for HIV-1 genomic RNA dimerization and packaging. Virology 375, 592–610.

Kageyama, S., Hoekzema, D.T., Murakawa, Y., Kojima, E., Shirasaka, T., Kempf, D.J., Norbeck, D.W., Erickson, J., Mitsuya, H., 1994. A C_2 symmetry-based HIV protease inhibitor, A77003, irreversibly inhibits infectivity of HIV-1 in vitro. AIDS Res. Hum. Retroviruses 10, 735–743.

Kaplan, A.H., Swanstrom, R., 1991. Human immunodeficiency virus type 1 Gag proteins are processed in two cellular compartments. Proc. Natl. Acad. Sci. U. S. A. 88, 4528–4532.

Kaplan, A.H., Zack, J.A., Knigge, M., Paul, D.A., Kempf, D.J., Norbeck, D.W., Swanstrom, R., 1993. Partial inhibition of the human immunodeficiency virus type 1 protease results in aberrant virus assembly and the formation of noninfectious particles. J. Virol. 67, 4050–4055.

Konvalinka, J., Litterst, M.A., Welker, R., Kottler, H., Rippmann, F., Heuser, A.M., Kräusslich, H.G., 1995. An active-site mutation in the human immunodeficiency virus type 1 proteinase (PR) causes reduced PR activity and loss of PR-mediated cytotoxicity without apparent effect on virus maturation and infectivity. J. Virol. 69, 7180–7186.

Kräusslich, H.G., 1991. Human immunodeficiency virus proteinase dimer as component of the viral polyprotein prevents particle assembly and viral infectivity. Proc. Natl. Acad. Sci. U. S. A. 88, 3213–3217.

Laughrea, M., Jetté, L., 1996. Kissing-loop model of HIV-1 genome dimerization: HIV-1 RNAs can assume alternative dimeric forms and all sequences upstream or downstream of hairpin 248–271 are dispensable for dimer formation. Biochemistry 35, 1589–1598.

Laughrea, M., Jetté, L., Mak, J., Kleiman, L., Liang, C., Wainberg, M.A., 1997. Mutations in the kissing-loop hairpin of human immunodeficiency virus type 1 reduce viral infectivity as well as genomic RNA packaging and dimerization. J. Virol. 71, 3397–3406.

Laughrea, M., Shen, N., Jetté, L., Darlix, J.-L., Kleiman, L., Wainberg, M.A., 2001. Role of distal zinc finger of nucleocapsid protein in genomic RNA dimerization of human immunodeficiency viryus type 1; no role for the palindrome crowning the R-U5 hairpin. Virology 281, 109–116.

Lener, D., Tanchou, V., Roques, B.P., Le Grice, S.F.J., Darlix, J.-L., 1998. Involvement of HIV-1 nucleocapsid protein in the recruitment of reverse transcriptase into nucleoprotein complexes formed in vitro. J. Biol. Chem. 273, 33781–33786.

Levin, J.G., Guo, J., Rouzina, I., Musier-Forsyth, K., 2005. Nucleic acid chaperone activity of HIV-1 nucleocapsid protein: critical role in reverse transcription and molecular mechanism. Prog. Nucleic Acid Res. Mol. Biol. 80, 217–286.

Ludtke, J.J., Sebestyen, M.G., Wolff, J.A., 2002. The effect of cell division on the cellular dynamics of microinjected DNA and dextran. Mol. Ther. 5, 579–588.

Mammano, F., Petit, S.C., Clavel, F., 1998. Resistance-associated loss of viral fitness in human immunodeficiency virus type 1: phenotypic analysis of protease and gag coevolution in protease inhibitor-treated patients. J. Virol. 72, 7632–7637.

Mervis, R.J., Ahmad, N., Lillehoj, E.P., Raum, M.G., Salazar, F.H., Chan, H.W., Venkatesan, S., 1988. The gag gene products of human immunodeficiency virus type 1: alignment within the gag open reading frame, identification of posttranslational modifications, and evidence for alternative gag precursors. J. Virol. 62, 3993–4002.

Mirambeau, G., Lyonnais, S., Coulaud, D., Hameau, L., Lafosse, S., Jeusset, J., Justome, A., Delain, E., Gorelick, E.J., Le Cam, E., 2006. Transmission electron microscopy reveals an optimal HIV-1 nucleocapsid aggregation with single-stranded nucleic acids and the mature HIV-1 nucleocapsid protein. J. Mol. Biol. 364, 496–511.

Moore, M.D., Fu, W., Soheilian, F., Nagashima, K., Ptak, R.G., Pathak, V.K., Hu, W.-S., 2008. Suboptimal inhibition of protease activity in human immunodeficiency virus type 1: effects on virion morphogenesis and RNA maturation. Virology 379, 152–160.

Mortuza, G.B., Haire, L.F., Stevens, A., Smerdon, S.J., Stoye, J., Taylor, I.A., 2004. High-resolution structure of a retroviral capsid hexameric amino-terminal domain. Nature 431, 481–485.

Pettit, S.C., Moody, M.D., Wehbie, R.S., Kaplan, A.H., Nantermet, P.V., Klein, C.A., Swanstrom, R., 1994. The p2 domain of human immunodeficiency virus type 1 Gag

regulates sequential proteolytic processing and is required to produce fully infectious virions. J. Virol. 68, 8017–8027.
Pettit, S.C., Henderson, G.J., Schiffer, C.A., Swanstrom, R., 2002. Replacement of the P1 amino acid of human immunodeficiency virus type 1 Gag processing sites can inhibit or enhance the rate of cleavage by the viral protease. J. Virol. 76, 10226–10233.
Pettit, S.C., Everitt, L.E., Choudhury, S., Dunn, B.M., Kaplan, A.H., 2004. Initial cleavage of the human immunodeficiency virus type 1 GagPol precursor by its activated protease occurs by an intramolecular mechanism. J. Virol. 78, 8477–8485.
Poon, D.T.K., Wu, J., Aldovini, A., 1996. Charged amino acid residues of human immunodeficiency virus type 1 nucleocapsid p7 protein involved in RNA packaging and infectivity. J. Virol. 70, 6607–6616.
Reicin, A.S., Ohagen, A., Yin, L., Hoglund, S., Goff, S.P., 1996. The role of Gag in human immunodeficiency virus type 1 virion morphogenesis and early steps of the viral life cycle. J. Virol. 70, 8645–8652.
Rose, R.B., Craik, C.S., Douglas, N.L., Stroud, R.M., 1996a. Three-dimensional structures of HIV-1 and SIV protease product complexes. Biochemistry 35, 12933–12944.
Rose, R.E., Gong, Y.-F., Greytok, J.A., Bechtold, C.M., Terry, B.J., Robinson, B.S., Alam, M., Colonno, R.J., Lin, P.-F., 1996b. Human immunodeficiency virus type 1 viral background plays a major role in development of resistance to protease inhibitors. Proc. Natl. Acad. Sci. U. S. A. 93, 1648–1653.
Rosé, J.R., Babé, L.M., Craik, C.S., 1995. Defining the level of human immunodeficiency virus type 1 (HIV-1) protease activity required for HIV-1 particle maturation and infectivity. J. Virol. 69, 2751–2758.
Schock, H.B., Garsky, V.M., Kuo, L.C., 1996. Mutational anatomy of an HIV-1 protease variant conferring cross-resistance to protease inhibitors in clinical trials. Compensatory modulations of binding and activity. J. Biol Chem. 271, 31957–31963.
Schwartz, M.D., Fiore, D., Panganiban, A.T., 1997. Distinct functions and requirements for the Cys-His boxes of the human immunodeficiency virus type 1 nucleocapsid protein during RNA encapsidation and replication. J. Virol. 71, 9295–9305.
Shehu-Xhilaga, M., Kraeusslich, H.G., Pettit, S., Swanstrom, R., Lee, J.Y., Marshall, J.A., Crowe, S.M., Mak, J., 2001. Proteolytic processing at the p2/nucleocapsid cleavage site is critical for human immunodeficiency virus type 1 RNA dimer maturation. J. Virol. 75, 9156–9164.
Sheng, N., Erickson-Viitanen, S., 1994. Cleavage of p15 protein in vitro by human immunodeficiency virus type 1 protease is RNA dependent. J. Virol. 68, 6207–6214.
Sheng, N., Pettit, S.C., Tritch, R.J., Ozturk, D.H., Rayner, M.M., Swanstrom, R., Erickson-Viitanen, S., 1997. Determinants of the human immunodeficiency virus type 1 p15NC-RNA interaction that affect enhanced cleavage by the viral protease. J. Virol. 71, 5723–5732.
Song, R., Kafaie, J., Yang, L., Laughrea, M., 2007. HIV-1 Viral RNA is selected in the form of monomers that dimerize in a three-step protease-dependent process; the DIS of stem-loop 1 initiates viral RNA dimerization. J. Mol. Biol. 371, 1084–1098.
Song, R., Kafaie, J., Laughrea, M., 2008. Role of the 5′ TAR stem-loop and the U5-AUG duplex in dimerization of HIV-1 genomic RNA. Biochemistry 47, 3283–3293.
Spiegel, M.R., 1961. Theory and problems of statistics. Schaum's outline series, McGraw Hill.
Tang, S., Murakami, T., Agresta, B.E., Campbell, S., Freed, E.O., Levin, J.G., 2001. Human immunodeficiency virus type 1 N-terminal capsid mutants that exhibit aberrant core morphology and are blocked in initiation of reverse transcription in infected cells. J. Virol. 75, 9366–9537.
Thomas, J.A., Gorelick, R.J., 2008. Nucleocapsid protein function in early infection processes. Virus Res. 134, 39–63.
Tozser, J., Blaha, I., Copeland, T.D., Wondrak, E.M., Oroszlan, S., 1991. Comparison of the HIV-1 and HIV-2 proteinases using oligopeptide substrates representing cleavage sites in Gag and Gag–Pol polyproteins. FEBS Lett. 281, 77–80.
Tseng, W.-C., Haselton, F.R., Giorgio, T.D., 1997. Transfection by cationic liposomes using simultaneously single cell measurements of plasmid delivery and transgene expression. J. Biol. Chem. 272, 25641–25647.
Vaughan, E.E., DeGiulio, J.V., Dean, D.A., 2006. Intracellular trafficking of plasmids for gene therapy: mechanisms of cytoplasmic movement and nuclear import. Curr. Gene Ther. 6, 671–681.
Veronese, F.D., Rahman, R., Copeland, T.D., Oroszlan, S., Gallo, R.C., Sarngadharan, M.G., 1987. Immunological and chemical analysis of p6, the carboxyl-terminal fragment of HIV p15. AIDS Res. Hum. Retroviruses 3, 253–264.
Von Schwedler, U.K., Stemmler, T.L., Klishko, V.Y., Li, S., Albertine, K.H., Davis, D.R., Sundquist, W.I., 1998. Proteolytic refolding of the HIV-1 capsid protein amino-terminus facilitates viral core assembly. EMBO J. 17, 1555–1568.
Von Schwedler, U.K., Stray, K.M., Garrus, J.E., Sundquist, W.I., 2003. Functional surfaces of the human immunodeficiency virus type 1 capsid protein. J. Virol. 77, 5439–5450.
Wang, S.-W., Aldovini, A., 2002. RNA incorporation is critical for retroviral particle integrity after cell membrane assembly of Gag complexes. J. Virol. 76, 11853–11865.
Wang, C.-T., Barklis, E., 1993. Assembly, processing and infectivity of human immunodeficiency virus type 1 gag mutants. J. Virol. 67, 4264–4273.
Wang, S.-W., Noonan, K., Aldovini, A., 2004. Nucleocapsid–RNA interactions are esssential to structural stability but not to assembly of retroviruses. J. Virol. 78, 716–723.
Wondrak, E.M., Louis, J.M., de Rocquigny, H., Chermann, J.-C., Roques, B.P., 1993. The gag precursor contains a specific HIV-1 protease cleavage site between the NC (p7) and p1 proteins. FEBS Lett. 333, 21–24.
Yu, X.-F., Matsuda, Z., Yu, Q.-C., Essex, M., 1995. Role of the C terminus Gag protein in human immunodeficiency virus type 1 virion assembly and maturation. J. Gen. Virol. 76, 3171–3179.
Zhang, Y.-M., Imamichi, H., Imamichi, T., Lane, H.C., Fallon, J., Vasudevachari, M.B., Salzman, N.P., 1997. Drug resistance during indinavir therapy is caused by mutations in the protease gene and in its gag substrate cleavages sites. J. Virol. 71, 6662–6670.
Zybarth, G., Krausslich, H.-G., Partin, K., Carter, C., 1994. Proteolytic activity of novel human immunodeficiency virus type 1 proteinase proteins from a precursor with a blocking mutation at the N-terminus of the PR domain. J. Virol. 68, 240–250.